HEFAT2014
10th International Conference on Heat Transfer, Fluid Mechanics and Thermodynamics
14 – 16 July 2014
Orlando, Florida

THE CHAOTIC BUBBLE DEPARTURES AS A RESULT OF NONLINEARITY OF GAS COMPRESSION IN THE PLENUM

Dzienis P., Mosdorf R.*
*Author for correspondence
Department of Mechanics and Applied Computer Science, Faculty of Mechanical Engineering,
Bialystok University of Technology,
Wiejska 45 C, 15-351 Bialystok,
Poland,
E-mail: r.mosdorf@pb.edu.pl

ABSTRACT

In the paper it has been analysed the influence of: nozzle diameter and height of liquid over the nozzle on the chaotic character of bubble departures. The analysis has been conducted based on the numerical model of chaotic bubble departures proposed in the paper [3]. The following forces in the model of bubble growth have been considered: drag force, Boussinesq–Basset force, added-mass forces and the changes in the gas momentum. The influence of Boussinesq–Basset and added-mass forces on the frequency of bubble departures has been discussed.

It has been shown that the intensity of appearance of the chaotic bubble departures is caused by increase in the nozzle diameter and height of liquid over the nozzle. The increase of the nozzle diameter causes the decrease of the bubble departure frequency and the depth of liquid penetration into the nozzle. It has also been shown that the increase of liquid height over the nozzle outlet modify the character of bubble departure. The increase of liquid height over the nozzle modify the frequency of bubble departure and depth of liquid penetration into the nozzle. Both forces: Boussinesq–Basset and added mass promote the bubble departures and decrease the depth of liquid penetration into the nozzle. The added mass force is greater than the Boussinesq–Basset force.

INTRODUCTION

There are a substantial number of papers that report the non-linear behaviours of the bubbling process [2, 3, 4, 5, 6, 7, 9]. The influence of the plate thickness, surface tension, the viscosity of the liquid and the height of the liquid over the nozzle on the depth of the liquid penetration into the nozzle has been reported in papers [1, 4, 7, 9].

The impact of the plenum volume and the height of the liquid over the orifice outlet on the frequency of the bubble departures have been investigated in the paper [1]. It has been observed that the increase in the plenum volume increases the time period between two subsequent bubbles [1]. The increase in the height of the liquid over the orifice outlet leads also to an increase in the time period between subsequent bubbles [9]. In paper [7] it has been found out that the time

NOMENCLATURE

C_d	[-]	Drag force coefficient
C_M	[-]	Added-mass force coefficient for a sphere
f	[Hz]	Frequency of bubble departure
g	[m/s^2]	Gravitational acceleration
h_w	[m]	Height of liquid column
l	[m]	Nozzle height
p_b	[Pa]	Pressure of the air inside the bubble
p_c	[Pa]	Gas pressure in the plenum chamber
p_h	[Pa]	Hydrostatic pressure
q	[m^3/s]	Air volume flow rate
q_b	[m^3/s]	Air volume flow rate supplied to the bubble
r	[m]	Radius of bubble
r_m	[m]	Radius of meniscus
r_n	[m]	Nozzle diameter
r_o	[m]	Bubble diameter
s	[m^2]	Cross-sectional area of the nozzle
t_0	[s]	Beginning of bubble movement
V_b	[m^3]	Volume of the bubble
V_c	[m^3]	Volume of plenum chamber
v_g	[m/s]	Gas velocity
v_l	[m/s]	Liquid velocity inside the nozzle
v_{pp}	[m/s]	Liquid velocity around growing bubble
x_c	[m]	Position of bubble centre
x_l	[m]	High of liquid penetration into the nozzle

Special characters

μ	[kg/ms]	Viscosity
μ_g	[kg/ms]	Gas dynamic viscosity
ρ	[kg/m^3]	Density
ρ_f	[kg/m^3]	Liquid density
σ	[N/m]	Surface tension

Subscripts

max	Maximum

period between the departing bubbles decreases when the number of gas-liquid interface oscillations decreases [9]. The phenomena of the liquid movement inside the orifice or nozzle have been experimentally investigated and modelled in papers [4, 8]. In the paper [4] the influence of the ration between the nozzle diameter and nozzle length on the depth of liquid penetration into the nozzle has been discussed. In the paper [8] the model of liquid penetration into the orifice has been proposed. The results of numerical analysis were compare with the experimental results presented in the paper [7].

The dynamics of bubble departures at a frequency of f = 3 Hz from a glass nozzle submerged in a tank filled with distilled water has been experimentally and theoretically studied in paper [3]. The volume of plenum chamber and the air volume flow rate were changed in the experiment. The air pressure, bubble paths and liquid flow inside the nozzle were simultaneously recorded using a data acquisition system and a high-speed camera. It was shown that an increase in the plenum chamber volume leads to an increase in the intensity of the occurrences of chaotic changes in the subsequent waiting times [3]. Examples of the recorded the depth of liquid penetration into the nozzle and pressure fluctuations [3] are shown in Fig. 1. The right side of Fig. 1 shows the system trajectory reconstruction in the space (p, h). The bubble growth creates a part of the trajectory where h = 0. The remaining part of the trajectory corresponds to the movement of liquid inside the nozzle.

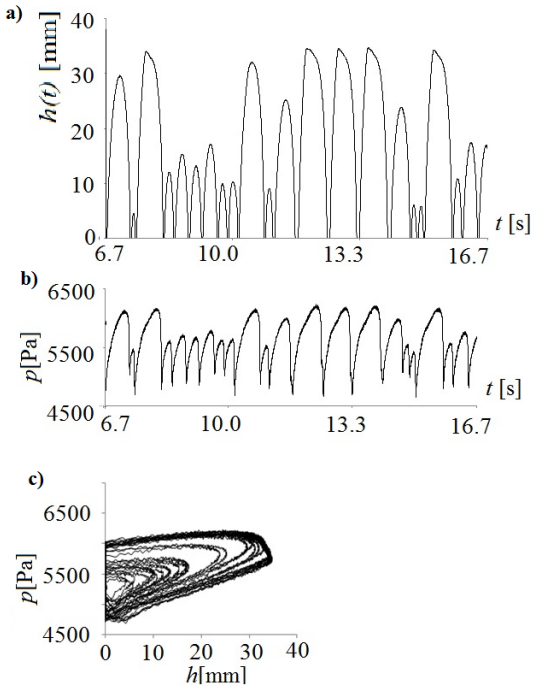

Figure 1 Experimental time series of the depth of the liquid penetration into the nozzle and the air pressure in the plenum chamber for gas with a volume flow rate of q = 0.00632 l/min plenum volume V = 10.45 ml. a) the depth of the liquid penetration into the nozzle, b) the air pressure in the plenum chamber, c) the system trajectory reconstruction in the space (p, h).

In the paper [3] the results of simulations based on the models of bubble growth and liquid flow inside the nozzle during the waiting time have been presented. It was shown that the air pressure rise, Δp_l, during the waiting time is a non-linear function of the gas pressure after the bubble departure and the liquid velocity around the nozzle outlet. The nonlinearity of Δp_l increases when the plenum chamber volume increases, and it decreases when the air volume flow rate increases [3].

In the present paper it has been analysed the influence of nozzle diameter and height of liquid over the nozzle outlet on the frequency of bubble departures and chaotic character of bubble departures. The analysis has been conducted based on the numerical model of chaotic bubble departures proposed in the paper [3]. The following forces in the model of bubble growth have been considered: drag force, Boussinesq–Basset force, added-mass forces and the changes in the gas momentum. The influence of Boussinesq–Basset and added-mass forces on the frequency of bubble departures has been discussed.

MODELING OF BUBBLE DEPARTURES

The model of subsequent bubble departures presented in the paper [3] was based on the model proposed by [8]. In the present paper the model was used for modelling the influence of: the plenum volume, nozzle diameter and height of liquid over the nozzle on the bubble departures frequency, depth of liquid movement into the nozzle and character (periodic or chaotic) of bubble departures. Forces considered in the model were as follows: the drag and added-mass forces, which are dependent on the liquid velocity around the nozzle outlet, buoyancy force, the surface tension force, Boussinesq–Basset force and the changes in the gas momentum

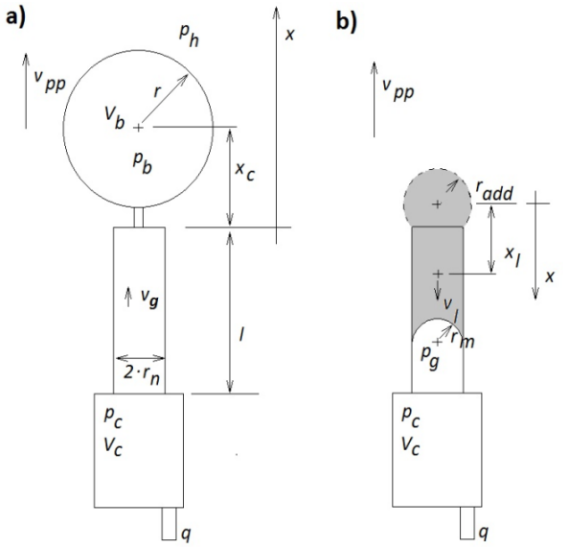

Figure 2 Schema of the model for the bubble growth and the liquid flow inside the nozzle. a) bubble growth, and b) liquid flow in the nozzle.

Figure 2 shows a schematic model of the bubble growth and the liquid flow in the nozzle. Equations (1 - 16) describe the bubble growth and the liquid movement inside the nozzle. The detail description of the model is presented in paper [3].

The bubble growth:

$$\frac{dp_b}{dt} = \left(\frac{p_b}{V_b}\right)\left[\left(\frac{\pi}{8\mu_g}\right)\left(\frac{r_n^4}{l}\right)\left(p_c - p_b\right) - \frac{dV_b}{dt}\right] \tag{1}$$

$$\frac{dp_c}{dt} = \frac{k_c p_c\left[q - \left(\frac{\pi}{8\mu_g}\right)\left(\frac{r_n^4}{l}\right)\left(p_c - p_b\right)\right]}{V_c} \tag{2}$$

$$r\left(\frac{d^2r}{dt^2}\right) - \left(\frac{3}{2}\right)\left(\frac{dr}{dt}\right)^2 = \left[\frac{p_b - p_h - \frac{2\sigma}{r} - 4\mu_l\frac{\left(\frac{dr}{dt}\right)}{r}}{\rho_l}\right] \tag{3}$$

When

$$F_B + F_M + F_{AM} - F_\sigma - F_d - F_{BB} > 0$$

then

$$\frac{d}{dt}\left[\left(\rho_g + C_b\rho_l\right)\cdot V_b\left(\frac{dx_c}{dt} - v_{pp}\right)\right] = F_B + F_M + F_{AM} - F_\sigma - F_d - F_{BB} \tag{4}$$

otherwise,

$x_c = r$
$v_c = d_r/d_t$

where

F_{AM} - added-mass force:

$$F_{AM} = -\left(\rho_g + C_b\rho_l\right)\frac{dV_b}{dt}\left(v_c - v_{pp}\right) \tag{5}$$

F_B - buoyancy force [11]:

$$F_B = g\left(\rho_l - \rho_g\right)\cdot V_b \tag{6}$$

F_M - gas momentum [10]:

$$F_M = \rho_g\frac{q_b^2}{\pi r_o^2} \text{ where } q_b = \left(\frac{\pi}{8\mu_g}\right)\left(\frac{r_n^4}{l}\right)\left(p - p_b\right) \tag{7}$$

F_σ - maximum value of the surface tension force:

$$F_\sigma = 2\pi\, r_n\sigma \tag{8}$$

when the cosine of the attachment angle is equal to 1,

F_d - drag force [12]:

$$F_d = 0.5C_d\rho_l\pi r^2\left(\frac{dx_c}{dt} - v_{pp}\right)\left|\frac{dx_c}{dt} - v_{pp}\right| \tag{9}$$

F_{BB} - Boussinesq–Basset force [11]:

$$F_{BB} = r^2\sqrt{\pi\rho_l\mu_l}\int_{t_0}^{t}\frac{\frac{dv_{x_c}}{d\tau}}{\sqrt{t-\tau}}d\tau \tag{10}$$

Criterion for bubble departure:

$$x_c >= r + 2r_n \tag{11}$$

The liquid movement:

$$\frac{dp_c}{dt} = \frac{p_c}{V_c}\left(q + \pi r_n^2\frac{dx_l}{dt}\right) \tag{12}$$

$$\frac{d}{dt}\left\{\left[0.5\rho_l\pi r_n^2 x_l + \rho_l\frac{4}{3}\pi\left(2r_n\right)^3\right]\frac{dx_l}{dt}\right\} = F_1 - F_2 \tag{13}$$

where

$$F_1 = -s\Delta p = -\pi r_n^2\left[p_c - \left(p_h + \rho_l g\left(2x_l\right) + 2\frac{\sigma}{r_n} - \frac{\rho v_{pp}\left|v_{pp}\right|}{2}\right)\right] \tag{14}$$

$$F_2 = 2*8\pi\mu_l x_l\frac{dx_l}{dt} \tag{15}$$

Criterion for the end of the liquid movement:

$$x_l < 0 \tag{16}$$

The time period of the bubble growth was divided into two stages: an increase in the spherical bubble radius described by the Rayleigh - Plesset equation [8] and the vertical movement of the spherical bubble described by the motion equation of the bubble centre, which includes the added-mass force [3]. The last phase of the bubble movement is shown in Fig. 2a. The vertical bubble motion is determined by Newton's second law (4). The equation of motion (4) considers added-mass force (5), the buoyancy force (6), the surface tension force (8), the drag force (9), Boussinesq–Basset force (10) and the change in the gas momentum (7). The air volume flow rate supplied to the bubble through the nozzle is determined by the Hagen-Poiseuille equation [8] and the pressure changes in the bubble

are described by equation (1), in which the isothermal process is considered. The pressure changes in the air supply system are described by equation (2). It has been assumed that the bubble is detached from the nozzle outlet when criterion (11) is fulfilled [8].

The model of the liquid flow inside the nozzle was based on the equation of motion of the mass centre of the liquid (13). The pressure changes in the air supply system are described by equation (12). The force F_1 (14) is related to the pressure difference that occurs in the system (with accounting for the changes in the dynamic pressure), and the force F_2 (15) is related to the resistance of the movement of the liquid in the nozzle. According to [8], the mass of the liquid that is involved in the movement caused by flooding the nozzle is greater than the mass of the liquid inside the nozzle. The weight of the liquid that is involved in the movement is equal to 0.5 of total mass of liquid inside the nozzle [8].

The set of equations (1-16) has been solved by using SCILAB. The ordinary differential equation solver (ODE) with root-finding capabilities has been used to make a determination of the time of the bubble growth and the waiting time. The relative and absolute tolerances were 10^{-5} and 10^{-7}.

The agreement of the simulation results with the measurement data has been tested in paper [3] - the good agreement between the experimental data and simulation has been obtained.

In the present paper it has been analysed the influence of the nozzle diameter and height of liquid over the nozzle on the frequency of bubble departures and chaotic character of bubble departures.

SIMULATION RESULTS

Changing the nozzle diameter

The simulation has been carried out for the following radiuses of nozzle diameter: 0.6 mm, 0.8 mm, 1 mm i 1.2 mm and plenum volume $V = 0.472$ ml, height of liquid over the nozzle $h_w = 0.49$ m and ait volume flow rate $q = 0.0078$ l/min. Depending on presence and absence of forces F_{BB} and F_{AM} four different types of simulations has been conducted.

In Figure 3a is presented the frequency of bubble departure vs. nozzle radius for different types of simulation. In Figure 3b is presented the maximum value of depth of liquid penetration into the nozzle. When the nozzle radius increases the frequency of bubble departures decreases (Figure 3a). The increases of the nozzle diameter causes also increases of the maximum depth of liquid penetration into the nozzle. Both forces F_{BB} and F_{AM} promote the bubble departures and decrease the depth of liquid penetration into the nozzle. The force F_{AM} is greater than the force F_{BB}.

Examples of the simulation results of the depth of liquid penetration into the nozzle and pressure fluctuations are shown in Fig. 4, where the data obtained for different nozzle diameter are presented. The right side of Fig. 4 shows the system trajectory reconstruction in the space (p, h) (the picture consisted of 30000 points). The bubble growth creates a part of the trajectory where $h = 0$. The remaining part of the trajectory corresponds to the movement of liquid inside the nozzle. During the periodic bubble departures, the subsequent trajectories are close to each other. In case of chaotic bubble departures the all trajectories are visible. We can note that the increase in the radius of nozzle lead to appearance the chaotic bubble departures.

Changing the height of liquid over the nozzle outlet

The simulation has been carried out for the following height of liquid over the nozzle outlet: 0.43m, 0.46m, 0.49m, 0.52m, volume of plenum chamber $V = 0.472$ ml, $r_n = 0.5$ mm and $q = 0.0078$ l/min. Depending on presence and absence of forces F_{BB} and F_{AM} four different types of simulations has been carried out.

In Figure 5a is presented the frequency of bubble departure vs. height of liquid over the nozzle. In Figure 5b is presented the maximum value of depth of liquid penetration into the nozzle. When the height of liquid over the nozzle increases the frequency of bubble departures changes wary small (Figure 5a). The increase of the height of liquid over the nozzle causes also small variation of the maximum depth of liquid penetration into the nozzle.

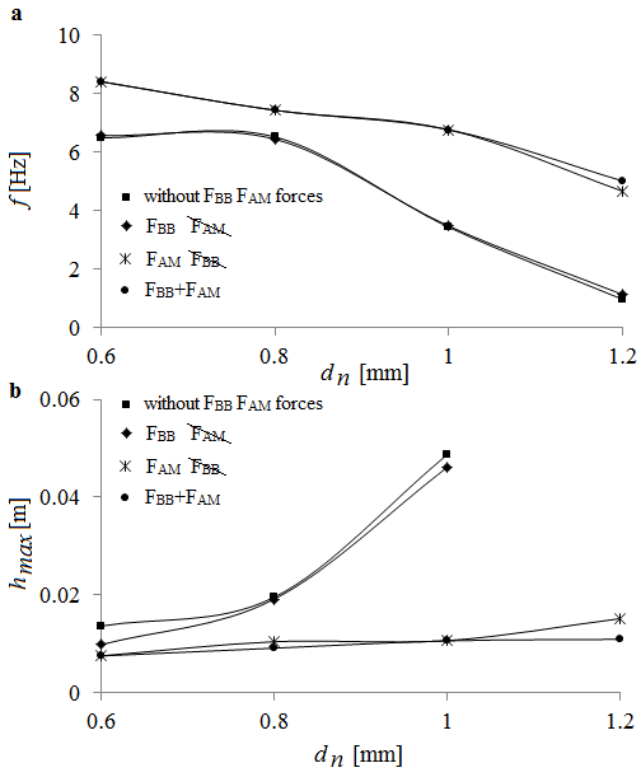

Figure 3 Frequency of bubble departures and maximum value of depth of liquid penetration into the nozzle vs. radius of nozzle for different types of simulations. a) frequency of bubble departures vs. radius of nozzle b) maximum value of depth of liquid penetration into the nozzle vs. radius of nozzle.

Examples of the simulation results of the depth of liquid penetration into the nozzle and pressure fluctuations are shown in Fig. 6, where the data obtained for different height of liquid over the nozzle are presented. The right side of Fig. 6 shows the system trajectory reconstruction in the space (p, h). We can note that the increase in the height of liquid over the nozzle modify the character of bubble departures.

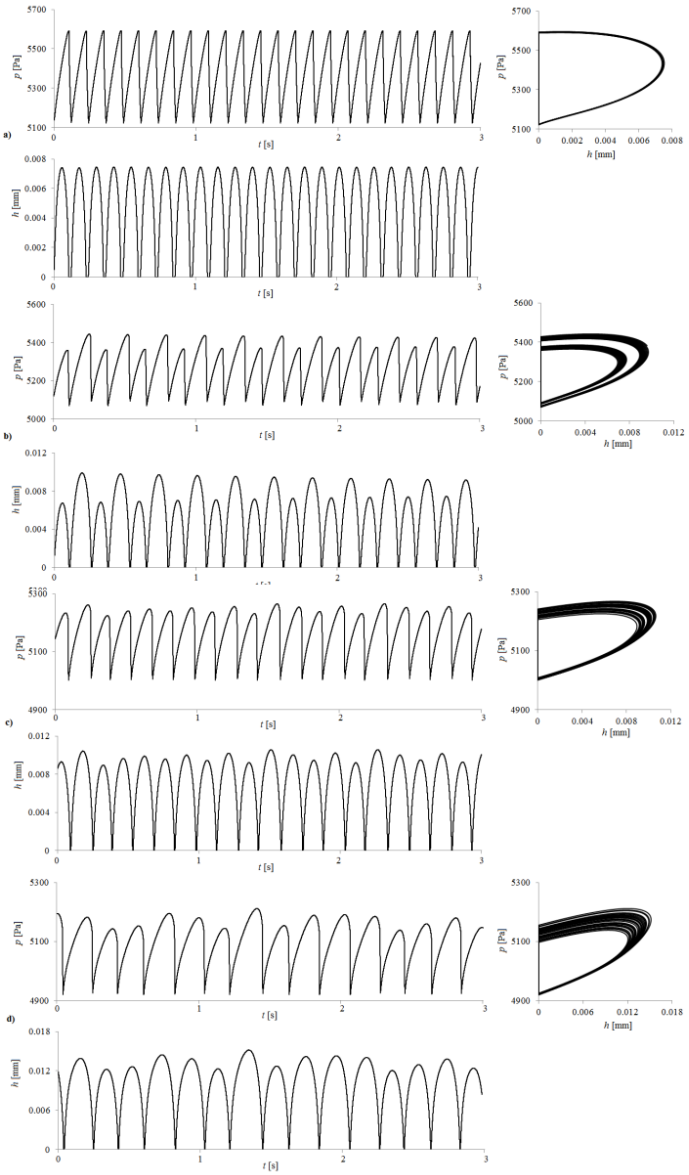

Figure 4 Examples of the simulation results of the depth of liquid penetration into the nozzle and pressure fluctuations. Charts in the right side of figure show the system trajectory reconstruction in the space (p, h). a) r_n = 0.6 mm, b) r_n = 0.8 mm, c) r_n = 1 mm, d) r_n = 1.2 mm.

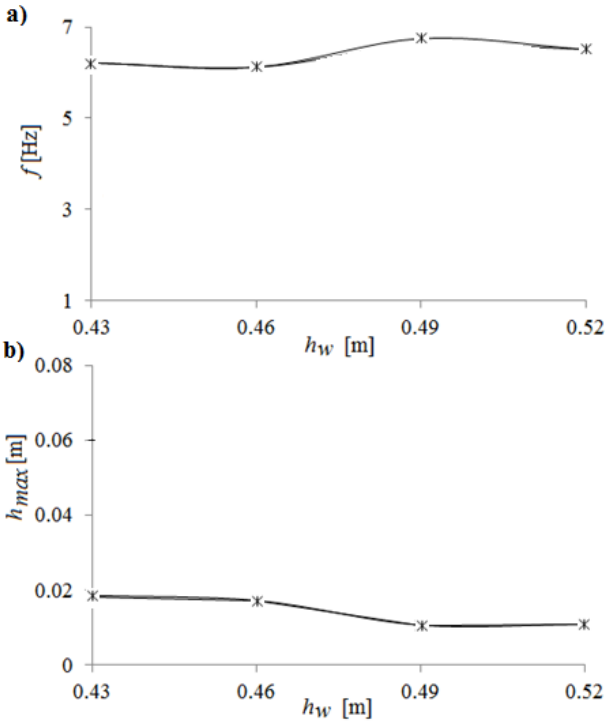

Figure 5 Frequency of bubble departures and maximum value of depth of liquid penetration into the nozzle vs. height of liquid over the nozzle. a) frequency of bubble departures vs. height of liquid over the nozzle b) maximum value of depth of liquid penetration into the nozzle vs. height of liquid over the nozzle.

To understand the mechanism of generation of chaotic bubble departures we analysed the influence of the small changes in the liquid velocity v_{pp} on the pressure changes Δp_l (v_{pp}, ...). The ranges in the pressure and liquid velocity changes in the simulations are similar to the ranges that appear in the simulation of non-periodic bubble departures. The air volume flow rate is equal to 0.009 l/min. In the analysis of the changes in $\Delta p_l(v_{pp}, ...)$, it has been assumed that $v_{ol} = v_{pp}$.

The changes in Δp_l as a function of v_{pp} are shown in Figure 7. The small increase in the liquid velocity v_{pp} leads to an increase in the values of Δp_l. The nonlinearity of the gas compression in the plenum increases with the increase radius of nozzle and high of liquid over the nozzle outlet.

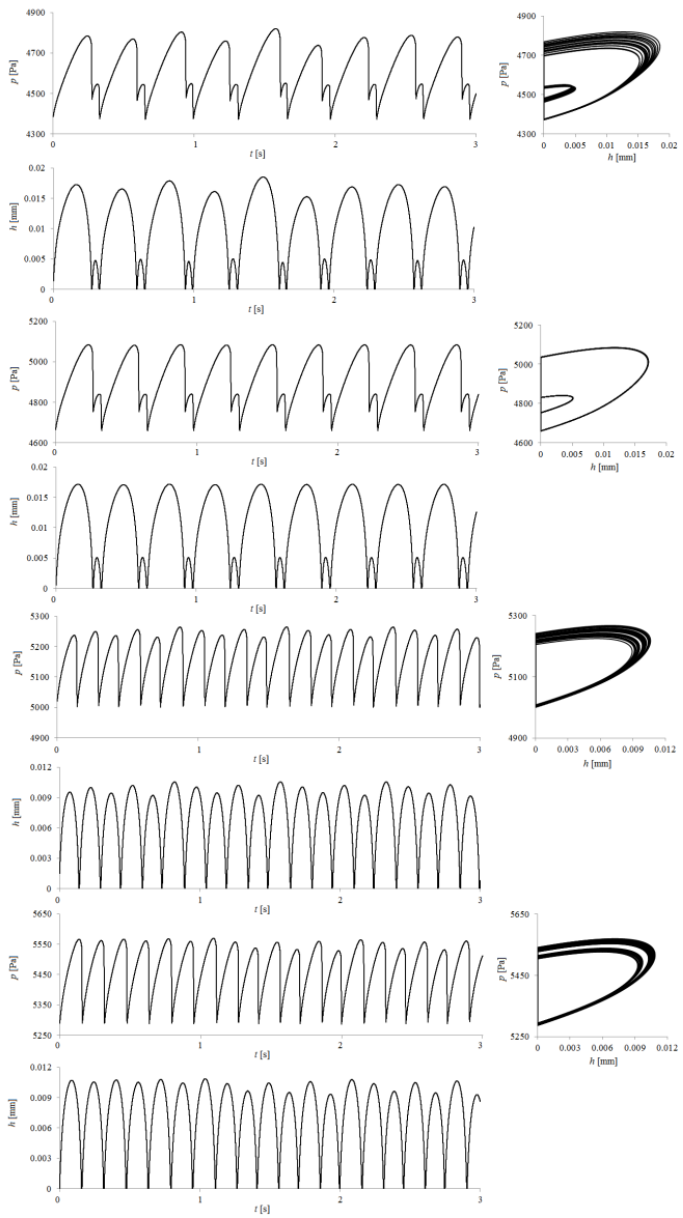

Figure 6 Examples of the simulation results of the depth of liquid penetration into the nozzle and pressure fluctuations. Charts in the right side of figure show the system trajectory reconstruction in the space (p, h). a) h_w = 0.43 m, b) h_w = 0.46 m, c) h_w = 0.49 m, d) h_w = 0.52 m.

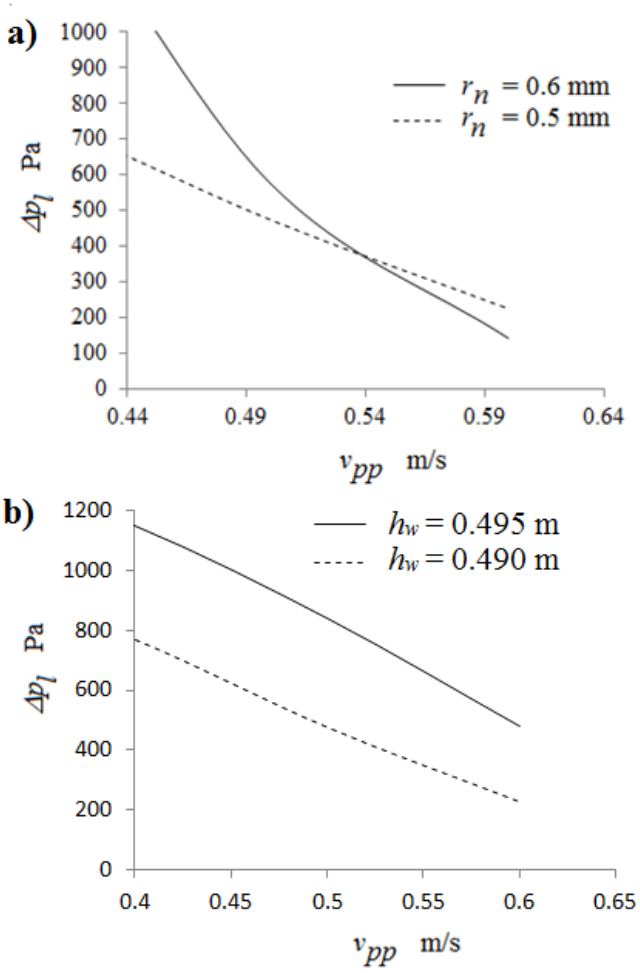

Figure 7 The changes in Δp_l as a function of v_{pp} for different high of liquid over the nozzle outlet and radius of nozzle. a) The changes in Δp_l as a function of v_{pp} for different radius of nozzle. b) The changes in Δp_l as a function of v_{pp} for different high of liquid over the nozzle outlet.

CONCLUSIONS

Changing the internal diameter of the nozzle modifies the frequency of bubble departures and the maximum depth of the fluid penetration into the nozzle. The increase of the nozzle diameter decreases the frequency of bubble departures. In this case the depth of liquid penetration into the nozzle increases. The increases of the nozzle internal diameter at a constant air flow rates leads to a chaotic bubble departures.

Changing the height of liquid over the nozzle (at constant air flow rates and nozzle diameter) modifies the depth of liquid penetration into the nozzle, the frequency of bubble departures. The modification of height of the liquid over the nozzle leads to the chaotic bubble departure.

It has been shown that the nonlinearity of the gas compression in the plenum increases with the increase of the radius of nozzle and high of liquid over the nozzle outlet. Such nonlinearity is responsible for the appearance of deterministic chaos in the simulations.

Both forces F_{BB} and F_{AM} promote the bubble departures and decrease the depth of liquid penetration into the nozzle. The force F_{AM} is greater than the force F_{BB}.

REFERENCES

[1] Antoniadis, D., Matzavinos, D., Stamatoudis, M., 1992. Effect of chamber volume and diameter on bubble formation at plated orifices. Chemical engineering research & design, Vol. 70, 161 - 165.

[2] Cieslinski, J.T., Mosdorf, R., 2005. Gas bubble dynamics experiment and fractal analysis. Int. J. Heat Mass Transfer 48 (9), 1808–1818.

[3] Dzienis P., Mosdorf R., 2014. Stability of periodic bubble departures at a low frequency. Chemical Engineering Science, article in press, http://dx.doi.org/10.1016/j.ces.2014.02.001

[4] Kovalchuk, V.I., Dukhin, S.S., Fainerman, V.B., Miller R., 1999. Hydrodynamic processes in dynamic bubble pressure experiments. 4. Calculation of magnitude and time of liquid penetration into capillaries. Colloids and Surfaces A: Physicochemical and Engineering Aspects 151, 525–536.

[5] Mosdorf, R., Shoji, M., 2003. Chaos in bubbling - nonlinear analysis and modeling. Chem. Eng. Sci. 58, 3837–3846.

[6] Mosdorf, R., Wyszkowski, T., 2011. Experimental investigations of deterministic chaos appearance in bubbling flow. International Journal of Heat and Mass Transfer. vol. 54, 5060-5069.

[7] Ruzicka, M.C., Bunganic, R. Drahos, J., 2009. Meniscus dynamics in bubble formation. Part I: Experiment. Chem. Eng. Res. Des. 87, 1349–1356.

[8] Ruzicka, M.C., Bunganic, R., Drahos, J., 2009b. Meniscus dynamics in bubble formation. Part II: Model. Chem. Eng. Res. Des. 87, 1357–1365.

[9] Stanovsky, P., Ruzicka, M.C., Martins, A., Teixeira, J.A., 2011. Meniscus dynamics in bubble formation: A parametric study. Chemical Engineering Science. 66, 3258–3267.

[10] Vazquez A., Leifer I., Sánchez R.M., 2010. Consideration of the dynamic forces during bubble growth in a capillary tube. Chemical Engineering Science, Volume 65, Issue 13, 4046-4054.

[11] Zhang J., Fan Liang-Shih., 2003. On the rise velocity of an interactive bubble in liquids. Chemical Engineering Journal 92, 169–176.

[12] Zhang, L., Shoji, M., 2001. Aperiodic bubble formation from a submerged orifice. Chemical Engineering Science 56, 5371-5381.